Supplementary figures

Figure S1.

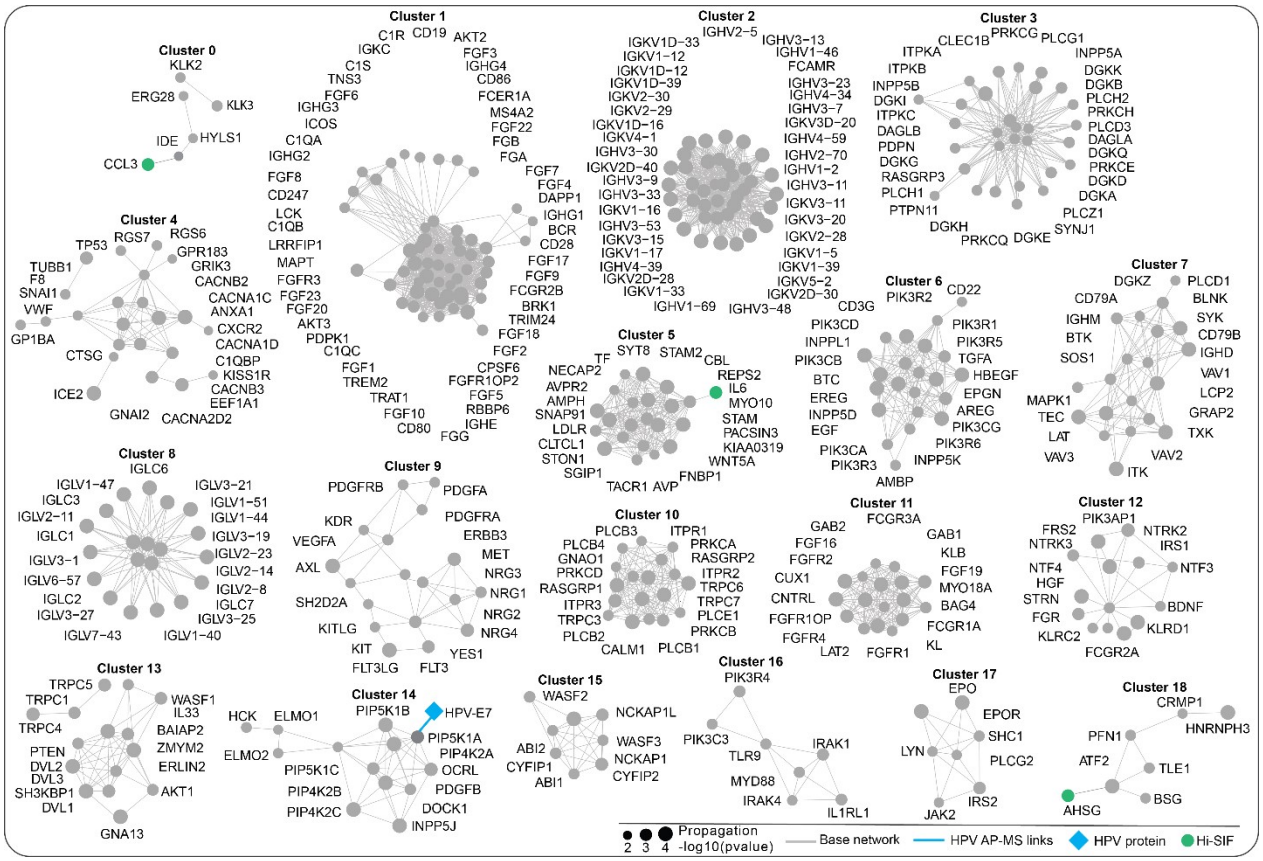

Fig. S1. Integrative propagation network for Hi-SIFs and HPV preys. Biological clusters from integrative Hi-SIFs/HPV network propagation analysis. The pathways associated with each cluster(s) are provided in Fig. 2C. Node size represents -log(*p*-value) from network propagation permutation test.

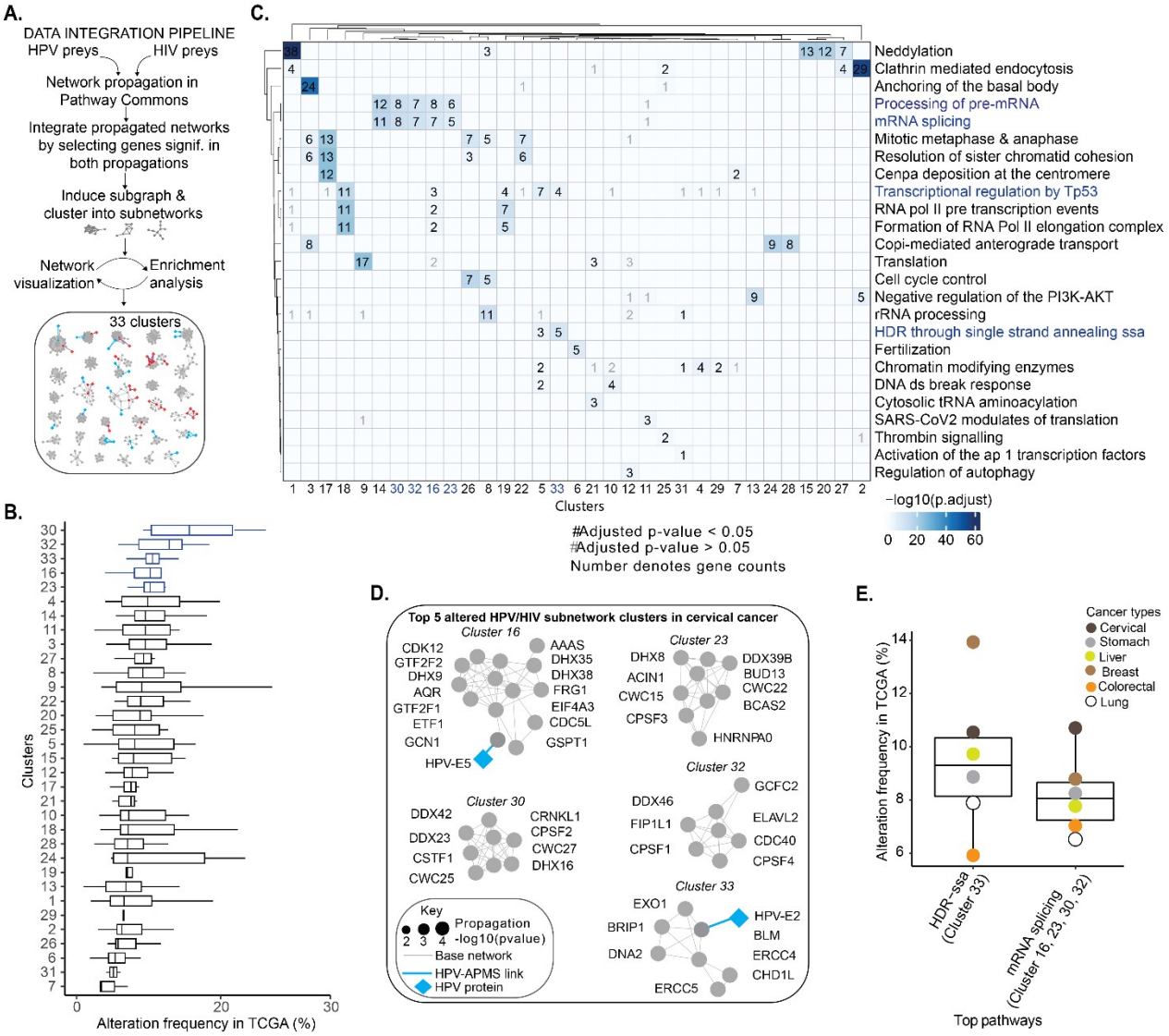

Fig. S2. Network propagation highlights biological pathways co-hijacked by HIV and HPV.

(A). Integrative network propagation pipeline for HPV and HIV preys. Using Pathway Commons for base network, network propagation was performed independently for the HIV and HPV preys. The propagated networks were integrated by selecting genes significant in both propagations to identify biological networks that are common between HPV and HIV. The top 500 significant genes from the propagation outputs were extracted, induced into subgraph, clustered into subnetworks followed by gene set ~~enrichment~~ over-representation analysis.

(B). Box plot showing the alteration frequencies (including point mutations, CNA and structural variants, gene and protein expression) of genes for each of the subnetwork clusters. The top five mutated subnetwork clusters (highlighted in blue) were selected for unbiased selection of pathway terms in (C). Data from cBioPortal.

(C). An enrichment heatmap obtained after gene set ~~enrichment~~ over-representation analysis of the integrated HPV/HIV propagated subnetwork clusters. The p-values were calculated by hypergeometric test with multiple hypothesis testing (FDR). The pathway terms associated with the top 5 altered clusters in cervical cancer patients from (B) are highlighted in blue. A complete set of enriched biological pathways is provided in Table S6.

(D). The top five altered subnetworks clusters identified in (B and C). All the 33 HPV/HIV propagated subnetwork clusters are shown in Fig. S3.

(E). Comparison of the alteration frequencies (including point mutations, CNA and structural variants, gene and protein expression) of nodes of the top five clusters grouped based on the pathways they are implicated in across common cancers among women. Data from cBioPortal.

Figure S2.

Figure S3.

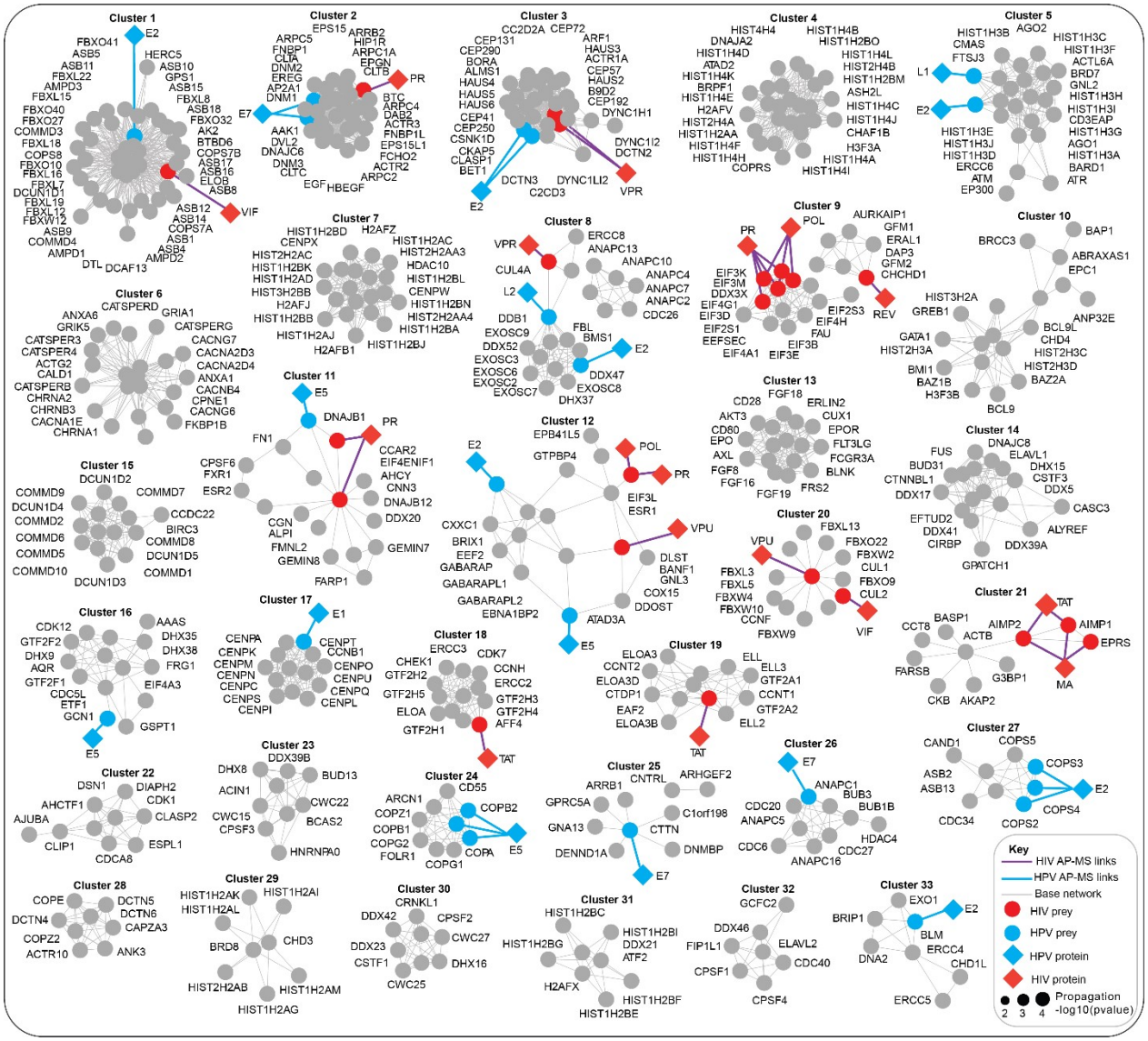

Fig. S3. Integrative propagation network for HIV and HPV preys. Biological clusters from integrative HIV/HPV network propagation analysis. The top pathway term associated with each of the subnetwork clusters are provided in Fig S2B. Node size depicts -log(p-value) from network propagation permutation test.

Figure S4.

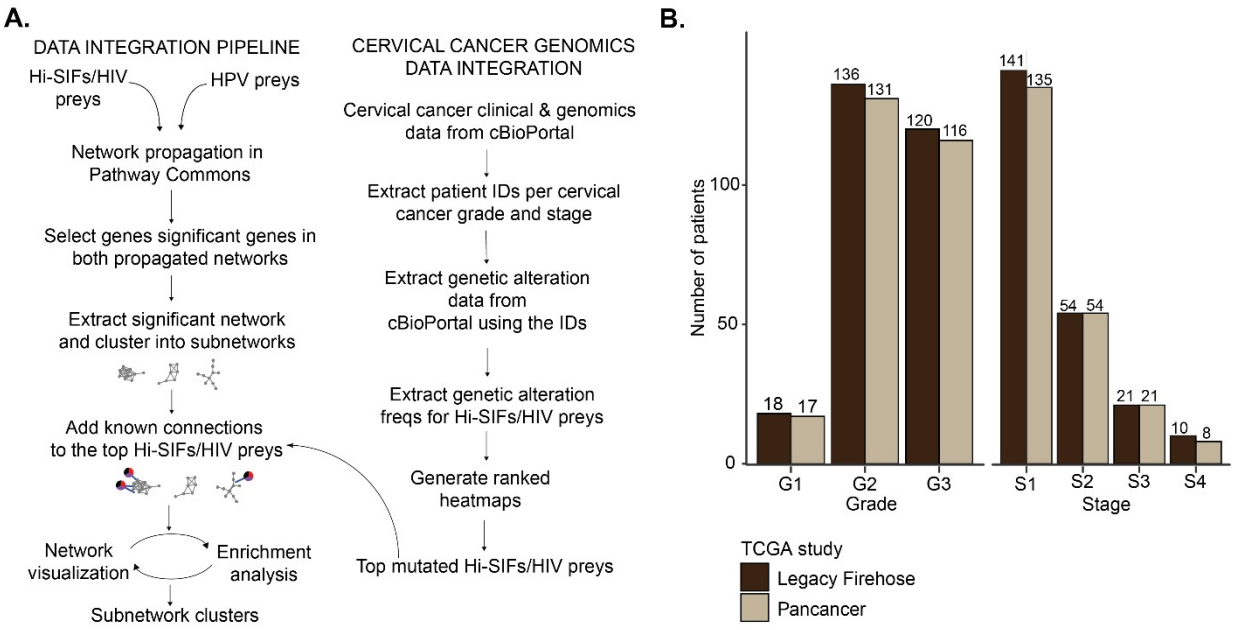

Fig. S4. Cervical cancer genomics data integration pipeline and TCGA patients utilized.
(A). Pipeline for integration of cervical cancer genomics data from cBioPortal into the HPV and Hi-SIFs or HIV propagated network. Cervical cancer genomic data were extracted from the cBioPortal and analysed to extract the top three mutated Hi-SIFs and HIV preys, which were then overlaid onto the integrative HPV and Hi-SIFs or HIV propagated networks to identify the pathways the top mutated Hi-SIFs or HIV preys are implicated in.
(B). The number of cervical cancer patients included in the analysis across different grades and stages from the two cervical cancer studies listed in the cBioPortal.

Figure S5.

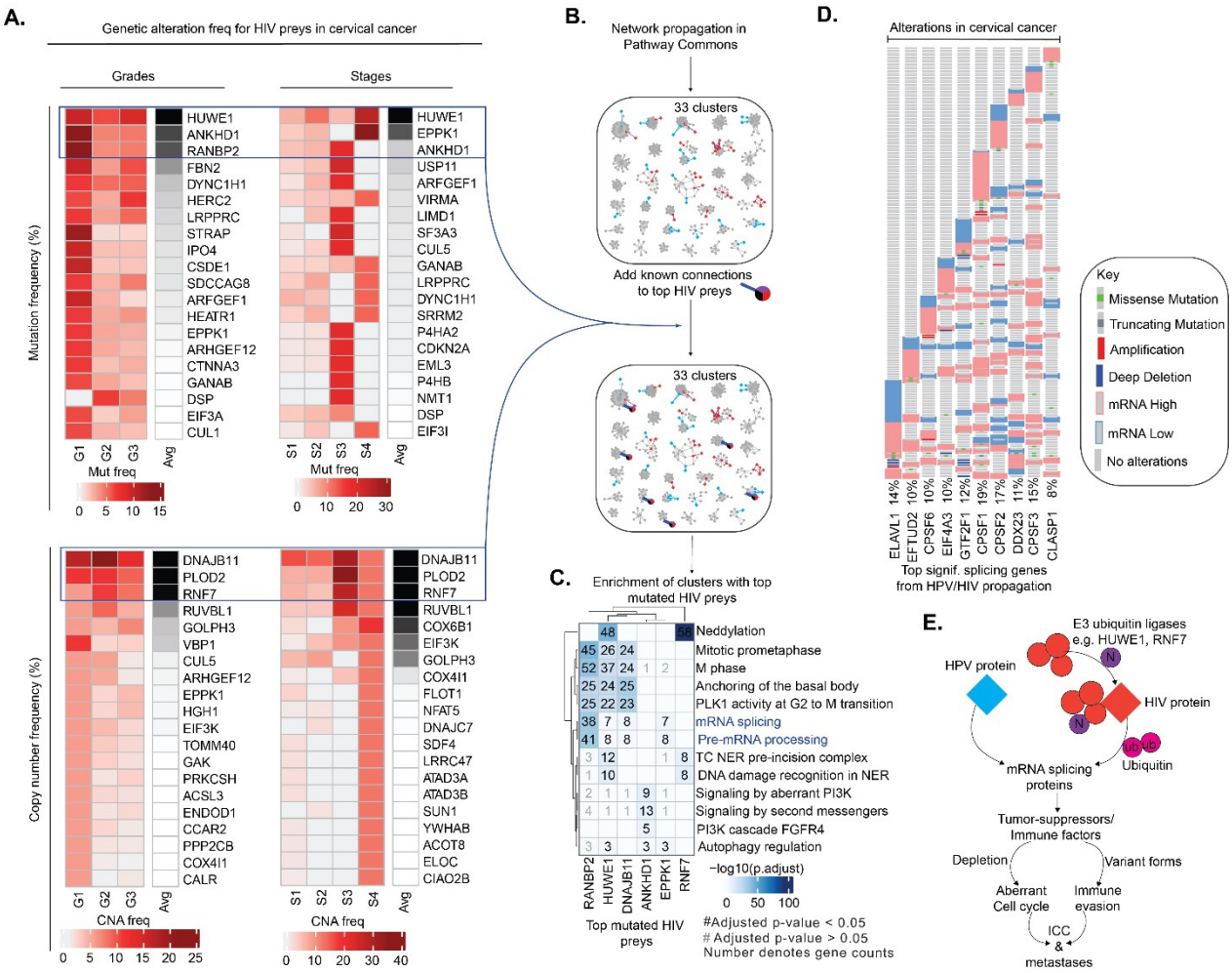

Fig. S5. Pathways converging between HIV, HPV and cervical cancer genomics.

(A). Ranked mutation and copy number alteration frequencies of HIV preys across different cervical cancer grades and stages from the cBioPortal and the top three preys that were selected for integration into the HIV/HPV propagated network.

(B). Integration of the top mutated HIV preys from the cBioPortal into the HIV/HPV propagated network. The top mutated HIV preys were overlaid onto the HIV/HPV propagated network by establishing known connections between them and the genes within the subnetwork clusters.

(C). Gene set ~~enrichment~~ over-representation analysis for propagated HIV-HPV subnetwork clusters with connections to the top mutated HIV preys. The pathways that are in line with the top five mutated clusters from Fig S2C are highlighted in blue. A complete set of enriched biological pathways for the HIV-HPV subnetwork clusters connected to the top mutated HIV preys are listed in Table S8.

(D). Oncoprint showing the alteration frequencies of the top ten significant mRNA splicing genes from HPV/HIV network propagation in cervical cancer. Each vertical grey column depicts a patient. The various genetic alterations recorded per patient for each of these ten genes are indicated at the bottom. About 63% of the cervical cancer patients undergo nonsynonymous mutations, structural variants and chromosomal CNA and alteration of mRNA expression in one or more of these ten genes. Data from cBioPortal.

(E). Model illustrating how HIV contributes to cervical cancer progression. E3 ubiquitin ligases are activated via neddylation and are utilized by HIV to ubiquitinate host restriction factors for proteasomal degradation. The activated E3 ligases may also ubiquitinate splicing proteins leading to depletion of certain proteins like tumor suppressors and/or may contribute to formation of variant proteins, resulting in deregulated cell cycle and immune evasion, respectively.

Figure S6.

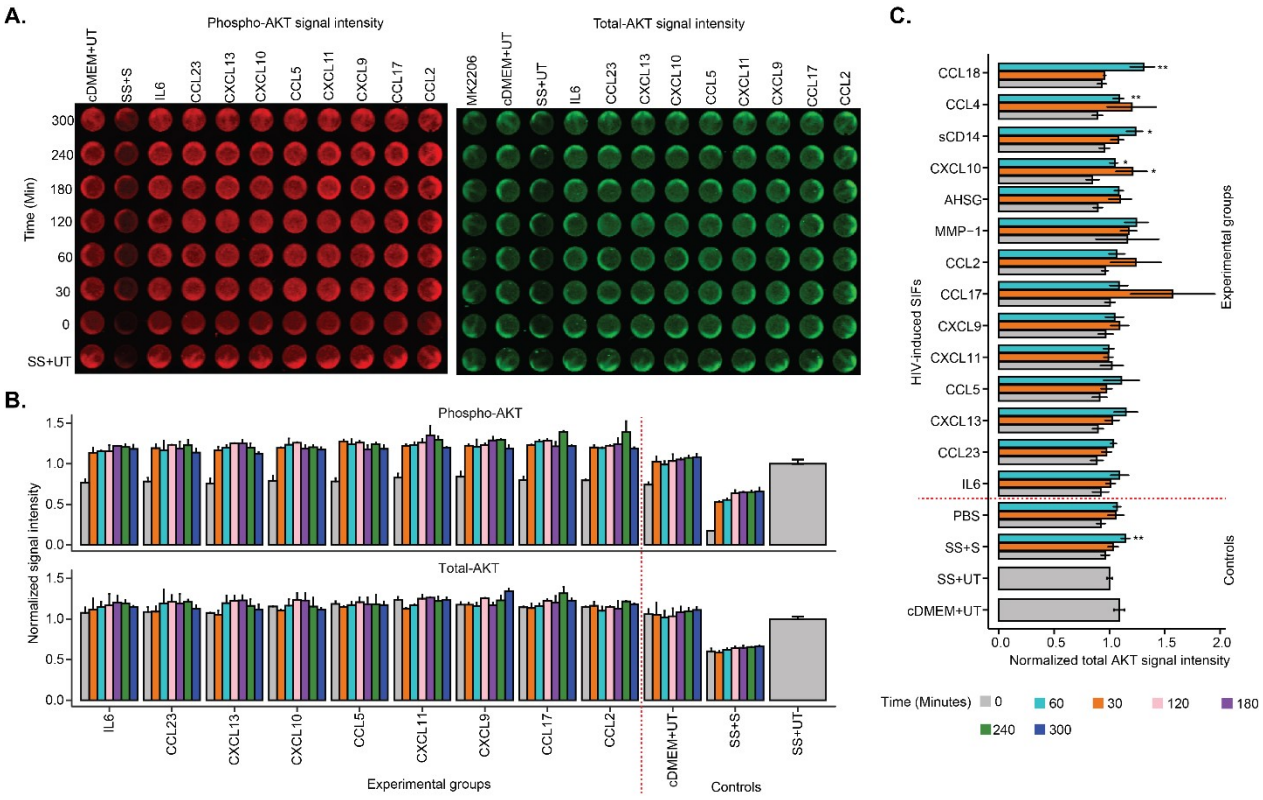

Fig. S6. Phospho- and total-AKT levels of cervical cells stimulated with Hi-SIFs at different time-points.
(A). Images showing intensity signals of different 96-plate wells stimulated with 9 different Hi-SIFs at time-points ranging from 0-300 min.
(B). Bar plots summarizing the signal intensities of the wells from Fig. S6A. Data represent mean ± standard error of two biological replicate plates.
(C). Levels of total-AKT as measured by in-cell Western analysis upon stimulation of C33A cells with Hi-SIFs. Bars depict the mean ± standard error of signal intensity of total-AKT normalized to levels of total-AKT of serum-starved cells per plate. Statistical comparisons between time 0 versus 30 or 60 min were performed using Wilcoxon test. Data represent technical duplicate wells per plate for three independent plates. The p-adjust are displayed. *, $p < 0.05$; **, $p < 0.01$.

Supplementary Tables

Table S1. A complete set of enriched biological pathways for HIV preys, Hi-SIFs, HPV preys and HPV-HIV overlapping preys.

Table S2. A complete set of enriched biological pathways for HPV/Hi-SIFs propagated subnetwork clusters.

Table S3. A complete set of enriched biological pathways for HIV preys propagated subnetwork clusters.

Table S4. A complete set of enriched biological pathways for Hi-SIFs preys propagated subnetwork clusters.

Table S5. A complete set of enriched biological pathways for HPV preys propagated subnetwork clusters.

Table S6. A complete set of enriched biological pathways for HPV/HIV preys propagated subnetwork clusters.

Table S7. A complete set of enriched biological pathways for the HPV/Hi-SIFs subnetwork clusters connected to the top mutated Hi-SIFs.

Table S8. A complete set of enriched biological pathways for the HPV/HIV subnetwork clusters connected to the top mutated HIV preys.

Table S9. Pathways common base network used for network propagation.

Table S10. Network propagation scores for HPV prey, Hi-SIFs and HPV preys.